IEEE Control Systems Letters paper presented at
2023 62nd IEEE Conference on Decision and Control (CDC)
December 13-15, 2023. Marina Bay Sands, Singapore

Linear Programming Approach to Relative-Orbit Control with Element-wise Quantized Control

Kazuya Echigo, Christopher R. Hayner, Avi Mittal, Selahattin Burak Sarsılmaz, Matthew W. Harris, and Behçet Açıkmeşe *Fellow, IEEE*

***Abstract*— This paper considers the problem of close-proximity relative-orbit control of spacecraft with control quantization constraints, models the problem as a mixed-integer program, and reformulates the problem as a linear program. The reformulation uses linearized relative orbital element dynamics with a sum-of-absolute-values objective, and it is proved that optimal controls for the reformulated problem satisfy the quantization constraint, that is, the quantization constraints are convexified for the reformulated continuous-time optimal control problem. This problem is then discretized, converted to a finite-dimensional linear program, and solved using commercially available convex optimization solvers with polynomial-time convergence guarantees. Since the mathematical proofs of convexification are available only for continuous-time case, their validity for discrete-time is demonstrated with extensive simulations. To this end, Monte Carlo simulations indicate that quantization is achieved with high probability while keeping spacecraft slew rates low relative to other proposed approaches.**

I. INTRODUCTION

This paper considers the problem of close-proximity relative-orbit control with control quantization constraints, as exemplified by on-orbit servicing. The need for quantized control is motivated by three propulsion system configurations: 1) a cluster of reaction control systems (RCS) using chemical thrusters, 2) multilevel unidirectional electric propulsion (EP) thrusters, and 3) modern hybrid propulsion systems [1]–[3]. NASA's Evolutionary Xenon Thruster (NEXT) propulsion system is an example of one that provides quantized control [4]. We investigate the case wherein the control is three-dimensional, and each component is required to belong to the finite set $\{0, \pm\frac{1}{m}u_{\max}, \ldots, \pm u_{\max}\}$ where $u_{\max}$ is a prescribed maximum control level and m is a prescribed natural number specifying the coarseness of the quantization. Each element of the set represents an admissible control value. Enforcement of the quantization constraint in an optimal control problem results in a non-convex problem. Finite-dimensional approximations of the optimal control problem for numerical purposes result in mixed-integer programs (MIPs) [5].

A brute-force approach to compute a MIP's globally optimal solution is to enumerate integer combinations, solve a convex optimization problem for each combination, and select the answer that minimizes the objective function. Algorithms such as branch-and-bound and branch-and-cut [6] often times provide efficient means of solving MIPs; however, worst-case complexity remains non-polynomial [7] and such algorithms are not currently suitable for onboard spacecraft implementations. The best off-the-shelf solvers, such as Gurobi [8], are designed to efficiently solve problems on the assumption that they can utilize multi-threading on many state-of-the-art processing cores, whereas computational resources available on spacecraft are restricted to a small number of low-powered processing cores.

In this paper, we propose a convex relaxation of the control set and use of a linear quantization-promoting objective function to generate a linear optimal control problem whose solutions satisfy the non-convex quantization constraint. Its discrete-time, finite-dimensional approximations can be solved as linear programs using efficient polynomial-time algorithms apt for spacecraft onboard usage [9].

The dynamical system considered describes the controlled orbital motion of a deputy spacecraft relative to a passive (coasting) chief spacecraft in a circular orbit. In the Hill frame, the linear time-invariant (LTI) equations of motion are known as the Clohessy-Wiltshire (CW) equations [10]. An alternative parameterization known as the modified linearized relative orbital elements (LROEs) is linear time-varying (LTV) and has an identically zero system matrix [11], [12]. In an optimal control setting, this fact renders the costate constant and facilitates a more direct proof of quantization.

It is known that L_1 norms promote sparsity and quantization [13]. An extension of the L_1 idea is the use of a sum-of-absolute-values (SOAV) objective, which promotes satisfaction of a prescribed quantization constraint. It has been proved that minimizing this objective generates control functions that satisfy the quantization constraint provided the dynamical system is LTI and satisfies strict assumptions about system structure [14]. The appearance of system structure requirements is not surprising as previous convex relaxations relied upon observability [15], [16], strong observability [17]–[19], and normality [20]. The needed system structure requirement fails to hold for both the CW and modified LROE systems. A key contribution of this paper is that the requirement is replaced with an easily checkable requirement on boundary conditions.

The remainder of the paper is organized as follows. Section II outlines the modified LROE to represent relative orbital dynamics as an LTV system. Section III introduces

The work was supported by Air Force Office of Scientific Research grant FA9550-20-1-0053 and by the Joint Center for Aerospace Technology Innovation Award. The authors are grateful to Drs. Trevor Bennett and Andrew Kitrell Kennedy for many helpful suggestions.

Kazuya Echigo, Christopher R. Hayner, Avi Mittal, and Behçet Açıkmeşe are with the William E. Boeing Department of Aeronautics and Astronautics, University of Washington, Seattle, WA 98195, USA. (e-mail: kazuyae@uw.edu). Selahattin Burak Sarsılmaz and Matthew W. Harris are with Utah State University, Logan, UT 84322, USA.

a SOAV objective function. Since it has been originally developed for the general LTI system in [14], the SOAV idea is adapted to the modified LROE system. Next, the main technical contributions are presented in Sections IV where it is proved that optimal solutions of the linear reformulation satisfy the quantization constraint. Finally, Section V presents Monte Carlo results to support the theoretical results and compare with common alternative approaches.

II. Overview of the Modified LROE

This section introduces the modified LROE-based LTV system formulation of the linearized relative equations of motion of a deputy spacecraft relative to a chief spacecraft in a circular orbit [11]. Analysis begins with the controlled CW equations [10], which are an LTI system describing the relative motion in a Hill frame. The mean motion (angular rate) of the chief's circular orbit is n. The CW equations are

$$\begin{aligned} \ddot{x}(t) - 3n^2 x(t) - 2n\dot{y}(t) &= u_1(t), \\ \ddot{y}(t) + 2n\dot{x}(t) &= u_2(t), \\ \ddot{z}(t) + n^2 z(t) &= u_3(t). \end{aligned} \tag{1}$$

The x coordinate describes relative motion measured from the chief spacecraft along its radius. The z coordinate describes the relative motion measured from the chief in the angular momentum direction of the circular orbit. Finally, the y coordinate describes the cross product of the z coordinate and the x coordinate, which completes the right-hand system. The relative control inputs in the coordinate directions are given by $u(t) = [u_1(t), u_2(t), u_3(t)]^\top$.

There is a rich literature on parameterizing this relative motion via relative orbital elements that match the integration constants of the CW equations and provide insight into the formation geometry [12], [21]. Among them, we prefer the modified LROE in [11] because they are a simple LTV system (4) with identically zero system matrix. In optimal control, this renders the costate constant and makes analysis of the control switching structure and synthesis of the optimal controls simpler.

The modified LROE consists of the following 6 variables

$$\text{æ} = \left[A_1, A_2, x_{\text{off}}, y_{\text{off}}, B_1, B_2\right]^\top, \quad \text{where} \tag{2}$$

$$\begin{aligned} A_1 &= -\frac{(3nx + 2\dot{y})\cos(nt) + \dot{x}\sin(nt)}{n}, \\ A_2 &= \frac{(3nx + 2\dot{y})\sin(nt) - \dot{x}\cos(nt)}{n}, \\ x_{\text{off}} &= 4x + \frac{2\dot{y}}{n}, \quad y_{\text{off}} = -\frac{2\dot{x}}{n} + y + (6nx + 3\dot{y})t, \\ B_1 &= z\cos(nt) - \frac{\dot{z}\sin(nt)}{n}, \; B_2 = -z\sin(nt) - \frac{\dot{z}\cos(nt)}{n}. \end{aligned} \tag{3}$$

As shown in [11], this yields the following LTV system

$$\dot{\text{æ}}(t) = B(t)u(t), \quad \text{where} \tag{4}$$

$$B(t) = \frac{1}{n}\begin{bmatrix} -\sin(nt) & -2\cos(nt) & 0 \\ -\cos(nt) & 2\sin(nt) & 0 \\ 0 & 2 & 0 \\ -2 & 3nt & 0 \\ 0 & 0 & -\sin(nt) \\ 0 & 0 & -\cos(nt) \end{bmatrix}. \tag{5}$$

It is a simple matter to show that, consistent with the CW system, the modified LROE system is 1) controllable and 2) not normal in the coordinate directions, i.e., the system is not controllable from each column of $B(t)$. Normality has been used previously to deduce quantization of optimal controls [14], [20], though our work shows normality is not necessary in the presence of our Assumption 4.1.

III. Problem Formulation

For a spacecraft equipped with orthogonally aligned thrusters, we address the problem of transferring from a specified initial condition to a specified final condition with quantized control input. Each element of $u(t)$ is required to satisfy the following quantization constraint:

$$u_j(t) \in \{0, \pm\frac{1}{m}U_j, \pm\frac{2}{m}U_j, \ldots, \pm U_j\}, \quad j = 1, 2, 3, \tag{6}$$

where $U_j > 0$ and $m \in \mathbb{N}$ are given. Note that the constraint set is disconnected and non-convex. Also, we assume a fixed final time $t_f > 0$ and boundary conditions $\text{æ}_0 = [A_{1,0}, A_{2,0}, x_{\text{off},0}, y_{\text{off},0}, B_{1,0}, B_{2,0}]^\top$ and $\text{æ}_f = [A_{1,f}, A_{2,f}, x_{\text{off},f}, y_{\text{off},f}, B_{1,f}, B_{2,f}]^\top$ are given.

In this paper, this non-convex feasibility problem is reformulated as an LP by introducing the sum-of-absolute-values (SOAV) objective function as in [14] whose integrand is

$$\phi(u(t)) = \sum_{j=1}^{3} L_j(u_j(t)), \quad \text{where} \tag{7}$$

$$L_j(u_j(t)) = \sum_{i=0}^{m} \omega_i \left(|u_j(t) - \frac{i}{m}U_{\text{j}}| + |u_j(t) + \frac{i}{m}U_{\text{j}}| \right), \tag{8}$$

with $\omega_0 \in \mathbb{R}$ being a positive weight constant and $\omega_i \in \mathbb{R}$, $i = 1, \ldots, m$ being non-negative weight constants that satisfy $\sum_{i=0}^{m} \omega_i = 1$. Fixing arbitrary $j \in \{1, 2, 3\}$, we can rewrite the piecewise linear function L_j as follows:

$$L_j(u_j(t)) = \begin{cases} -a_k u_j(t) + 2a'_k, & \text{if } u_j(t) \in [-\frac{k}{m}U_j, -\frac{k-1}{m}U_j], \\ 2\sum_{i=0}^{m} \omega_i \frac{i}{m}U_{\text{j}}, & \text{if } u_j(t) = 0, \\ a_k u_j(t) + 2a'_k, & \text{if } u_j(t) \in [\frac{k-1}{m}U_j, \frac{k}{m}U_j], \end{cases} \tag{9}$$

where

$$a_k = 2\sum_{i=0}^{k-1} \omega_i, \; a'_k = \sum_{i=k}^{m} \omega_i \frac{i}{m}U_{\text{j}}, \quad k = 1, \ldots, m. \tag{10}$$

The key feature of this function is that, as shown in the next section, it promotes a quantized control. Introducing it yields the following optimal control problem.

Problem 1:

$$\begin{aligned} \min_u \; & \int_0^{t_f} \phi(u(t))dt \\ \text{s.t. } & \dot{\text{æ}}(t) = B(t)u(t), \quad |u_j(t)| \le U_j, \; j = 1, 2, 3 \\ & \text{æ}(0) = \text{æ}_0, \; \text{æ}(t_f) = \text{æ}_f. \end{aligned}$$

After discretization of the time domain, the finite-dimensional approximation of this optimal control problem

is an LP. Since LPs can be solved to global optimality with polynomial-time interior-point methods (IPMs), this formulation has significant computational advantages over a non-convex, integer-based approach [22].

In the next section, we will show that any solution to Problem 1 satisfies the aforementioned non-convex quantization constraint, i.e., the control inputs solving Problem 1 take the predetermined quantized values in (6). However, before proceeding to this proof, existence of an optimal solution is shown. Note that the control constraints are convex, the matrix-valued function B is continuous, the objective function is continuous and convex, and all boundary conditions are specified. All conditions of Corollary 5.1 in [23, p. 67] are satisfied. Therefore, an optimal solution exists whenever a feasible one exists.

IV. Proofs for the Quantized Control

This section proves that any optimal solution to Problem 1 satisfies the non-convex quantization constraint (6). We first introduce a version of the maximum principle [23, pp. 185-186] tailored to Problem 1 and in a convenient form for use in proving Theorems 4.2 and 4.3. Consider the following general optimal control problem:

$$\begin{aligned}\min_{u} \ & \int_0^{t_f} \ell(t,u(t))dt \\ \text{s.t. } & \dot{y}(t) = f(t,u(t)),\ y(t)\in\mathcal{Y} \text{ and } u(t)\in\mathcal{U}, \\ & y(0)=y_0 \text{ and } y(t_f)=y_f.\end{aligned}$$

The time domain of the problem is the non-degenerate interval $I=[0,t_f]$. The state trajectory y is absolutely continuous, the control input u is measurable, and the functions ℓ and f satisfy some regularity conditions (see Assumption 3.1 in [23, p. 183]). The Hamiltonian for this problem is given by

$$\mathcal{H}(t,u(t),\lambda_0,\lambda) = \lambda_0\ell(t,u(t)) + \lambda^\top f(t,u(t)). \tag{11}$$

With this, necessary conditions for optimality can be stated.

Theorem 4.1 (Pontryagin's Maximum Principle): If u^* and y^* are the optimal control and state trajectories, then there exist a scalar constant $\lambda_0\in\{0,-1\}$ and an absolutely continuous vector function λ such that the following conditions are satisfied:

1) Almost everywhere on I:

$$\dot{\lambda} = -\frac{\partial H}{\partial y}(t,u^*,\lambda_0,\lambda) = 0. \tag{12}$$

Thus, λ is constant.

2) Almost everywhere on I:

$$\mathcal{H}(t,u^*(t),\lambda_0,\lambda) \geq \mathcal{H}(t,u(t),\lambda_0,\lambda)\ \ \forall u(t)\in\mathcal{U} \tag{13}$$

3) $(\lambda,\lambda_0)\neq 0$.

The second item is called the pointwise maximum condition. The third item is called the non-triviality condition.

A. Useful Properties

This subsection introduces a fundamental notation and a lemma that are used throughout the remainder of the paper. We first introduce the following notation for simplicity:

$$\begin{aligned} b_1(t) &= -\frac{1}{n}[\sin(nt),\cos(nt),0,2]^\top, \\ b_2(t) &= \frac{1}{n}[-2\cos(nt),2\sin(nt),2,3nt]^\top, \\ b_3(t) &= -\frac{1}{n}[\sin(nt),\cos(nt)]^\top. \end{aligned} \tag{14}$$

Also, we introduce the following lemma and proof regarding a function being zero on a set of positive measure.

Lemma 4.1: Let $a,b,c,d\in\mathbb{R}$ and $p: I\to\mathbb{R}$ given by

$$p(t) = a\sin(nt) + b\cos(nt) + ct + d. \tag{15}$$

Let $J\subset I$ have positive measure. If $p=0$ on J, then $p=0$ on I and $a=b=c=d=0$.

Proof: The function p is analytic, from which it follows that $p=0$ on I. The function p is a linear combination of linearly independent functions on the vector space of real-valued functions. Hence, $a=b=c=d=0$. ■

B. Theorem and Proof that u_1 and u_2 are quantized

With the optimality conditions stated, we now introduce the main technical result of this paper in Theorem 4.2 and 4.3, which prove that the optimal solution to Problem 1 takes quantized values. Since Problem 1 can be completely decomposed into two optimization problems, Theorem 4.2 and 4.3 deal with these two optimization problems respectively. The following assumption is also made for Theorem 4.2. It is reasonable since typical proximity operations occur over a few orbits, and x_{off} is often assumed to be zero to avoid the secular increase of $y(t)$ in the Hill frame [24].

Assumption 4.1:

$$[A_{1,f},A_{2,f},x_{\text{off},f},y_{\text{off},f}] \neq [A_{1,0},A_{2,0},x_{\text{off},0},y_{\text{off},0}], \tag{16}$$

$$|y_{\text{off},f}-y_{\text{off},0}| < \tfrac{3U_2}{m}\left(\left(\tfrac{t_f}{2}\right)^2 - \left(\tfrac{2}{3n}\right)^2\right), \tag{17}$$

$$x_{\text{off},f} = x_{\text{off},0}, \tag{18}$$

$$\tfrac{3}{4}nt_f > 1. \tag{19}$$

Theorem 4.2: Under Assumption 4.1, $u_1^*(t)$ and $u_2^*(t)$ in Problem 1 satisfy (6) a.e. on I.

Proof: The objective function, dynamics, and constraints associated with u_1 and u_2 are decoupled from u_3. Hence, u_1^* and u_2^* from Problem 1 is equivalent to u_1^* and u_2^* in the following problem.

Problem 2:

$$\begin{aligned}\min_{u_1,u_2} & \int_0^{t_f}\sum_{j=1}^{2} L_j(u_j(t))dt \\ \text{s.t. } & \dot{x}(t) = \sum_{j=1}^{2} b_j(t)u_j(t),\ |u_j(t)|\leq U_{\text{j}}\ \ j=1,2, \\ & x(0) = [A_{1,0},A_{2,0},x_{\text{off},0},y_{\text{off},0}]^\top, \\ & x(t_f) = [A_{1,f},A_{2,f},x_{\text{off},f},y_{\text{off},f}]^\top,\end{aligned}$$

where $x(t) \in \mathbb{R}^4$ is the first four elements of $\text{æ}(t)$. Now we show that $u_1^*(t)$ and $u_2^*(t)$ in Problem 2 take quantized values. The Hamiltonian for Problem 2 is given by

$$\mathcal{H}(t, u(t), \lambda_0, \lambda) = \lambda_0 \sum_{j=1}^{2} L_j(u_j(t)) + \lambda^\top \sum_{j=1}^{2} b_j(t) u_j(t). \tag{20}$$

In this proof, the vector $\lambda \in \mathbb{R}^4$ is defined as $\lambda = [a, b, c, d]^\top$. The remainder of the proof addresses the two cases: $\lambda_0 = 0$ and $\lambda_0 = -1$.

(Case 1: $\lambda_0 = 0$) With $\lambda_0 = 0$, the pointwise maximum condition implies that $u_j^*(t) \in \{-U_j, U_j\}$ provided that $\lambda^\top b_j(t) \neq 0$ a.e. on I, i.e., the control is quantized. To show that this is indeed the situation, two subcases are explored. In the first subcase, suppose there exists $J \subset I$ with positive measure such that $n\lambda^\top b_1(t) = 0$ on J. Therefore,

$$-a\sin(nt) - b\cos(nt) - 2d = 0 \text{ on } J. \tag{21}$$

By Lemma 4.1, $a = b = d = 0$. From the non-triviality condition, it is concluded that $c \neq 0$ such that $n\lambda^\top b_2(t) = 2c \neq 0$. The pointwise maximization condition implies that

$$u_2^*(t) = \begin{cases} +U_2, & c > 0 \\ -U_2, & c < 0 \end{cases} \quad \text{a.e. on } I. \tag{22}$$

Inspection of the equations of motion reveals that this control violates (18) in Assumption 4.1. Hence, the first subcase is impossible.

In the second subcase, suppose there exists $J \subset I$ with positive measure such that $n\lambda^\top b_2(t) = 0$ on J. Therefore,

$$-2a\cos(nt) + 2b\sin(nt) + 2c + 3dnt = 0 \text{ on } J. \tag{23}$$

By Lemma 4.1, $a = b = c = d = 0$. This violates the non-triviality condition, and the second subcase is impossible. Hence, the optimal control is quantized when $\lambda_0 = 0$.

(*Case 2*: $\lambda_0 = -1$) With $\lambda_0 = -1$, the pointwise maximum condition implies that $u_j^*(t)$ satisfies (6) provided that $\lambda^\top b_j(t) \neq \pm a_k$ a.e. on I. To show this, we first let $\mathcal{H}_j(t, u_j(t), \lambda_0, \lambda) = \lambda_0 L_j(u_j(t)) + \lambda^\top b_j(t) u_j(t)$, $j = 1, 2$. Clearly, $\mathcal{H} = \mathcal{H}_1 + \mathcal{H}_2$. For $\lambda_0 = -1$, we substitute (9) into $\mathcal{H}_j$ and then provide the maximizer of $\mathcal{H}_j$, that is, the optimal control $u_j^*(t)$, as in [14]:

$$\arg\max_{u_j(t)} \mathcal{H}_j(t, u_j(t), \lambda_0, \lambda) = \begin{cases} [\frac{k-1}{m}U_j, \frac{k}{m}U_j], & \text{if } \lambda^\top b_j(t) = a_k, \\ [-\frac{k}{m}U_j, -\frac{k-1}{m}U_j], & \text{if } \lambda^\top b_j(t) = -a_k, \\ U_\text{j}, & \text{if } a_m < \lambda^\top b_j(t), \\ \frac{k'-1}{m}U_j, & \text{if } a_{k'-1} < \lambda^\top b_j(t) < a_{k'}, \\ 0, & \text{if } -a_1 < \lambda^\top b_j(t) < a_1, \\ -\frac{k'-1}{m}U_j, & \text{if } -a_{k'} < \lambda^\top b_j(t) < -a_{k'-1}, \\ -U_\text{j}, & \text{if } \lambda^\top b_j(t) < -a_m, \end{cases} \tag{24}$$

where $k = 1, \ldots, m$ and $k' = 2, \ldots, m$. Consequently, the pointwise maximum condition generates a quantized control except possibly when the following three subcases occur.

In the first subcase, suppose there exists $J \subset I$ with positive measure such that $\lambda^\top b_1(t) = a_k$ on J. Therefore,

$$a\sin(nt) + b\cos(nt) + 2d + na_k = 0 \text{ on } J. \tag{25}$$

By Lemma 4.1, $\lambda^\top b_1(t) = a_k$ on I, $a = b = 0$, and $d = -\frac{n}{2}a_k$. Substituting them into $\lambda^\top b_2(t)$ gives

$$\lambda^\top b_2(t) = -\frac{3}{2}na_k t + \frac{2c}{n}, \quad \text{and} \tag{26}$$

$$\lambda^\top b_2(0) - \lambda^\top b_2(t_f) = \frac{3}{2}na_k t_f > 2a_k \geq 2a_1, \tag{27}$$

where the first inequality follows from (19) in Assumption 4.1. Note that $\lambda^\top b_2$ is an affine decreasing function on I. If $\lambda^\top b_2(t) \leq a_1$ on I, due to (27), there is an interval with positive measure such that $\lambda^\top b_2(t) < -a_1$ on that interval. In conjunction with the maximizer of $\mathcal{H}_j$ and the equations of motion, this violates (18). Similarly, it is also impossible that $\lambda^\top b_2(t) \geq -a_1$ on I. If $\lambda^\top b_2(t) > a_1$ on a positive measure interval and $\lambda^\top b_2(t) < -a_1$ on another positive measure interval, then (18) requires $\lambda^\top b_2$ to be symmetric with respect to the point $(\frac{t_f}{2}, 0)$ and u_2^* to be symmetric with respect to the same point a.e. on I. It yields $c = \frac{3}{8}t_f n^2 a_k$. Letting $t_\alpha \in [0, \frac{t_f}{2})$ be such that $\lambda^\top b_2(t_\alpha) = a_1$, we have

$$\begin{aligned} y_{\text{off},f} - y_{\text{off},0} &= \int_0^{t_f} 3tu_2^*(t)dt - \int_0^{t_f} \frac{2}{n}u_1^*(t)dt \\ &\leq \int_0^{t_\alpha} 3(2t - t_f)u_2^*(t)dt \\ &\leq \int_0^{t_\alpha} 3(2t - t_f)\frac{U_2}{m}dt. \end{aligned} \tag{28}$$

The first inequality follows from the facts that $u_1^*(t) \geq 0$ a.e. on I, $u_2^*(t) = 0$ a.e. on $(t_\alpha, t_f - t_\alpha)$, and u_2^* is symmetric with respect to $(\frac{t_f}{2}, 0)$ a.e. on I. Furthermore, on $[0, t_\alpha)$, $u_2^*(t) \geq \frac{U_2}{m}$ a.e. and $2t - t_f$ is negative, which gives the second inequality. Lastly, we have

$$t_\alpha = \frac{t_f}{2} - \frac{2a_1}{3na_k} \geq \frac{t_f}{2} - \frac{2}{3n} > 0, \tag{29}$$

where the equality is a consequence of $\lambda^\top b_2(\frac{t_f}{2}) = 0$ and $\lambda^\top b_2(t_\alpha) = a_1$, the first inequality follows from the fact that $a_k \geq a_1$ for $k = 1, \ldots, m$, and the second inequality is due to (19). The result of the last integral in (28) is $3\frac{U_2}{m}(t_\alpha^2 - t_f t_\alpha)$, which is a convex quadratic function in t_α. Under the constraint in (29) and $t_\alpha < \frac{t_f}{2}$, it attains its maximum at $t_\alpha = \frac{t_f}{2} - \frac{2}{3n}$. Therefore,

$$y_{\text{off},f} - y_{\text{off},0} \leq -\frac{3U_2}{m}\left(\left(\frac{t_f}{2}\right)^2 - \left(\frac{2}{3n}\right)^2\right), \tag{30}$$

which violates (17) in Assumption 4.1. Hence, the first subcase is impossible.

In the second subcase, suppose there exists $J \subset I$ with positive measure such that $\lambda^\top b_1(t) = -a_k$ on J. As with the first subcase, this also violates (17) in Assumption 4.1. Hence, the second subcase is impossible.

In the third subcase, suppose there exists $J \subset I$ with positive measure such that $\lambda^\top b_2(t) = \pm a_k$ on J. Therefore,

$$-2a\cos(nt)+2b\sin(nt)+(2c\pm na_k)+3dnt = 0 \text{ on } J. \quad (31)$$

By Lemma 4.1, $\lambda^\top b_2(t) = \pm a_k$ on I, $a = b = d = 0$, and $c = \pm\frac{n}{2}a_k$. Hence, $u_2^*(t)$ is either non-negative or non-positive a.e on I. This, together with (18) in Assumption 4.1, imply that $u_2^*(t) = 0$ a.e. on I. Furthermore, $\lambda^\top b_1(t) = 0$ on I, which implies that $u_1^*(t) = 0$ a.e. on I. Therefore, $u_1^*(t)$ and $u_2^*(t)$ are zero a.e. on I. It violates (16) in Assumption 4.1, and the third subcase is impossible. Hence, the optimal control is quantized when $\lambda_0 = -1$. ∎

C. Theorem and Proof that u_3 is quantized

We now turn our attention to $u_3(t)$ in Problem 1 and introduce the following theorem stating that the optimal solution $u_3^*(t)$ of Problem 1 satisfies the quantization constraint.

Theorem 4.3: The optimal control $u_3^*(t)$ in Problem 1 satisfies (6) a.e. on I.

Proof: The proof is similar to the one in the previous section. The objective function, dynamics, and constraints associated with u_3 are decoupled from u_1 and u_2. Hence, u_3^* from Problem 1 is equivalent to u_3^* in the following problem.

Problem 3:

$$\begin{aligned}&\min_{u_3} \int_0^{t_f} L_3(u_3(t))dt\\ &\text{s.t. } \dot{x}(t) = b_3(t)u_3(t),\ |u_3(t)| \le U_3,\\ &\quad x(0) = [B_{1,0}, B_{2,0}]^\top,\ x(t_f) = [B_{1,f}, B_{2,f}]^\top,\end{aligned}$$

where $x(t) \in \mathbb{R}^2$ is the last two elements of $\text{æ}(t)$ and t_f is fixed. The Hamiltonian for Problem 3 is given by

$$\mathcal{H}(t, u_3(t), \lambda_0, \lambda) = \lambda_0 L_3(u_3(t)) + \lambda^\top b_3(t)u_3(t). \quad (32)$$

In this proof, the vector $\lambda \in \mathbb{R}^2$ is defined as $\lambda = [e, f]^\top$. The remainder of the proof addresses the two cases: $\lambda_0 = 0$ and $\lambda_0 = -1$.

(*Case 1*: $\lambda_0 = 0$) With $\lambda_0 = 0$, the pointwise maximum condition implies that $u_3^*(t) \in \{-U_3, U_3\}$ provided that $\lambda^\top b_3(t) \neq 0$ a.e. on I, i.e., the control is quantized. To show that this is indeed the situation, suppose there exists $J \subset I$ with positive measure such that

$$n\lambda^\top b_3(t) = -e\sin(nt) - f\cos(nt) = 0 \text{ on } J. \quad (33)$$

It follows from Lemma 4.1 that $e = f = 0$. This violates the non-triviality condition, and this case is impossible. Hence, the optimal control is quantized when $\lambda_0 = 0$.

(*Case 2*: $\lambda_0 = -1$) With $\lambda_0 = -1$, the pointwise maximum condition implies that $u_3^*(t)$ satisfies (6) provided that $\lambda^\top b_3(t) \neq \pm a_k$ a.e. on I. To show this, suppose there exists $J \subset I$ with positive measure and index k such that $\lambda^\top b_3(t) = \pm a_k$ on J. It follows from Lemma 4.1 that $e = f = 0$ and $a_k = 0$. This violates $a_k > 0$, and this case is impossible. Hence, the optimal control satisfies the quantization constraint when $\lambda_0 = -1$. ∎

V. NUMERICAL RESULTS

The theoretical results hold in a continuous-time setting. For efficient numerical solution, Problem 1 is discretized (as done in [15]–[20]) resulting in a finite-dimensional linear program solvable with IPMs. Given that quantization is not guaranteed in the finite-dimensional setting, the performance of this approach is demonstrated statistically in a Monte Carlo analysis. Optimization is done using the convex optimization solver ECOS [25] in Python.

The approach is compared with two popular alternatives: the L_1 problem with integrand $|u_1(t)| + |u_2(t)| + |u_3(t)|$, which is a special case of Problem 1, and the minimum energy problem with integrand $u_1^2(t) + u_2^2(t) + u_3^2(t)$. The L_1 problem is known to promote control quantization of a bang-bang nature (large changes in control values between nodes). The minimum energy problem is known to promote non-quantized control with small changes between nodes.

We discretize all problems with a zero-order hold on the control and time step $\Delta t = 50\,\text{s}$. The Monte Carlo analysis consists of $50\,000$ feasible problems (samples) with randomized boundary conditions divided into 50 batches with each batch containing a random time of flight (TOF) between $4000\,\text{s}$ to $28\,000\,\text{s}$. The TOF is fixed within each batch but randomized between the batches. The initial condition is fixed: $\text{æ}_0 = 0$. The components of æ_f are sampled from a uniform distribution given by $[-800, 800]\,\text{m}$ such that Assumption 4.1 is satisfied. The other fixed parameters are given by

$$\begin{aligned}m = 3,\ U_{\max} := U_1 = U_2 = U_3 = 1\times10^{-5}\,\text{m/s}^2,\\ n = 1.106\times10^{-3}\,\text{s}^{-1},\ \omega_0 = \omega_1 = \omega_2 = \omega_3 = 0.25. \quad (34)\end{aligned}$$

For each trial, time is non-dimensionalized by t_f, control input by $U_{\max}$, and state vector by $\frac{U_{\max}}{n^2}$.

As an example, Figure 1 shows the solution of Problem 1 in the trial whose æ_f is $[60, 0, 0, 50, 0, 0]^\top\,\text{m}$ and t_f is $8000\,\text{s}$. Performance of the approach is quantified in two ways. First, the quantization success rate is analyzed. If the distance from $u_j(t_k)$ to its closest quantized value in (6) is less than 1% of $U_{\max}$ for every $j \in \{1, 2, 3\}$, the node t_k is labeled "quantization holds." The success rate for a given sample is defined by dividing the number of labeled nodes in the control profile by the total number of nodes in the sample. Table I shows the quantization success rate distributions for the three approaches. The mean quantization success rates of Problem 1 and the L_1 problem are both 98%, whereas that of the minimum energy problem is less than 1%. The results of Problem 1 and the L_1 problem imply that, in each trial, quantization fails approximately 2% of the time. It is due to discretization, which was highlighted in prior studies using the maximum principle [15], [16].

Second, the slew rate is analyzed [26]. The slew rate measures the change in control between nodes, and it is calculated by dividing the infinity norm of changes in u between temporal nodes by Δt. Table I shows the means of the maximum slew rates in each trial. Minimizing L_1 leads to quantization but typically at higher slew rates. Minimizing

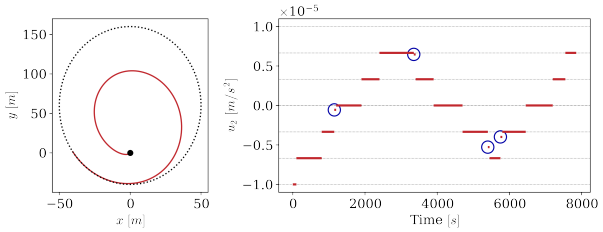

Fig. 1. Hill frame trajectory (left) and a representative control profile $u_2(t)$ (right) from Problem 1. The left displays the top view of the trajectory (red), $\mathscr{E}_0$ (black dot), and the unforced trajectory with initial value $\mathscr{E}_f$ (black dotted ellipse). The right displays desirable quantization values (black dotted lines) and the control profile (red lines). The control inputs circled in blue do not satisfy the quantized constraint.

TABLE I

QUANTIZATION SUCCESS RATES AND SLEW RATES DISTRIBUTIONS

	Quantization Success Rate				**Mean of the**
	Min	Max	Std Dev*	Mean	**Max Slew Rates**
Problem	[%]	[%]		[%]	$[10^{-8}\ \mathrm{m/s^3}]$
Problem 1	91.4	99.6	1.0	98.0	7.0
L_1	93.7	99.4	1.0	98.0	20
Min Energy	0	73.6	4.5	0.81	1.9

* Standard Deviation.

energy leads to lower slew rates but not quantization. Consequently, these results show that the proposed approach has two advantages: 1) quantization and 2) lower slew rates.

VI. CONCLUSION

The problem of close-proximity relative-orbit control with an element-wise control quantization constraint was investigated. Despite the quantization constraint being non-convex, a linear programming formulation of the problem was presented leading to an efficient numerical solution using IPMs. Proofs that solutions of the linear formulation satisfy the constraint were based on continuous-time optimal control and relied upon an assumption on boundary conditions. Because numerical methods solve a discrete-time approximation of the problem, quantization is not guaranteed in practice. Despite this fact, Monte Carlo simulations indicate that quantization is achieved numerically with high probability. The slew rates, or changes between quantization levels, were also low as appropriate for electric propulsion systems. In conclusion, the linear formulation provides an efficient, practical means of solving the orbit transfer problem with control quantization.

REFERENCES

[1] A. Axelrod, M. Guelman, and D. Mishne, "Optimal control of interplanetary trajectories using electrical propulsion with discrete thrust levels," *Journal of Guidance, Control, and Dynamics*, vol. 25, no. 5, pp. 932–939, 2002.

[2] J. M. Knittel, J. A. Englander, M. T. Ozimek, J. A. Atchison, and J. J. Gould, "Improved propulsion modeling for low-thrust trajectory optimization," in *AAS/AIAA Space Flight Mechanics Meeting*, Feb 2017.

[3] I. Napoli and M. Pontani, "Discrete-variable-thrust guidance for orbital rendezvous based on feedback linearization," *Aerotecnica Missili & Spazio*, vol. 101, no. 4, pp. 351–360, Dec. 2022.

[4] M. Patterson, J. Foster, T. Haag, V. Rawlin, G. Soulas, and R. Roman, "Next: Nasa's evolutionary xenon thruster," in *38th AIAA/ASME/SAE/ASEE Joint Propulsion Conference & Exhibit*.

[5] A. Bemporad and M. Morari, "Control of systems integrating logic, dynamics, and constraints," *Automatica*, vol. 35, no. 3, pp. 407–427, 1999.

[6] M. Padberg and G. Rinaldi, "A branch-and-cut algorithm for the resolution of large-scale symmetric traveling salesman problems," *SIAM Review*, vol. 33, no. 1, pp. 60–100, 1991.

[7] B. Guenin, J. Könemann, and L. Tunçel, *A Gentle Introduction to Optimization*. Cambridge University Press, 2014.

[8] Gurobi Optimization, LLC, "Gurobi Optimizer Reference Manual," 2022. [Online]. Available: https://www.gurobi.com

[9] D. Dueri, B. Açıkmeşe, D. Scharf, and M. W. Harris, "Customized real-time interior-point method for onboard powered descent guidance," *Journal of Guidance, Control and Dynamics*, vol. 40, pp. 197–212, 2017.

[10] H. D. Curtis, *Orbital Mechanics for Engineering Students: Revised Reprint*. Butterworth-Heinemann, 2021.

[11] T. Bennett and H. Schaub, "Continuous-time modeling and control using nonsingular linearized relative-orbit elements," *Journal of Guidance, Control, and Dynamics*, vol. 39, no. 12, pp. 2605–2614, 2016.

[12] J. Sullivan, S. Grimberg, and S. D'Amico, "Comprehensive survey and assessment of spacecraft relative motion dynamics models," *Journal of Guidance, Control, and Dynamics*, vol. 40, no. 8, pp. 1837–1859, 2017.

[13] M. Nagahara, D. E. Quevedo, and D. Nešić, "Maximum hands-off control: A paradigm of control effort minimization," *IEEE Transactions on Automatic Control*, vol. 61, no. 3, pp. 735–747, 2016.

[14] T. Ikeda, M. Nagahara, and S. Ono, "Discrete-valued control of linear time-invariant systems by sum-of-absolute-values optimization," *IEEE Transactions on Automatic Control*, vol. 62, no. 6, pp. 2750–2763, 2017.

[15] B. Açıkmeşe and L. Blackmore, "Lossless convexification of a class of optimal control problems with non-convex control constraints," *Automatica*, vol. 47, no. 2, pp. 341–347, 2011.

[16] L. Blackmore, B. Açıkmeşe, and J. M. Carson, "Lossless convexification of control constraints for a class of nonlinear optimal control problems," *Systems & Control Letters*, vol. 61, no. 8, pp. 863–870, 2012.

[17] M. W. Harris and B. Açıkmeşe, "Lossless convexification of non-convex optimal control problems for state constrained linear systems," *Automatica*, vol. 50, no. 9, pp. 2304–2311, 2014.

[18] N. T. Woodford and M. W. Harris, "Geometric properties of time-optimal controls with state constraints using strong observability," *IEEE Transactions on Automatic Control*, vol. 67, no. 12, pp. 6881–6887, 2022.

[19] S. Kunhippurayil and M. Harris, "Strong observability as a sufficient condition for non-singularity and lossless convexification in optimal control with mixed constraints," *Control Theory & Tech.*, 2022.

[20] M. W. Harris, "Optimal control on disconnected sets using extreme point relaxations and normality approximations," *IEEE Transactions on Automatic Control*, vol. 66, no. 12, pp. 6063–6070, 2021.

[21] S. D'Amico, "Relative orbital elements as integration constants of hill's equations," *German Space Operations Center (DLR/GSOC) TN 05–08*, Dec 2005.

[22] S. Boyd and L. Vandenberghe, *Convex Optimization*. Cambridge University Press, 2004.

[23] L. D. Berkovitz, *Optimal Control Theory*. Springer-Verlag, 1975.

[24] H. Schaub and J. L. Junkins, *Analytical Mechanics of Space Systems*, 4th ed. Reston, VA: AIAA Education Series, 2018.

[25] A. Domahidi, E. Chu, and S. Boyd, "Ecos: An socp solver for embedded systems," in *2013 European Control Conference (ECC)*, 2013, pp. 3071–3076.

[26] R. Saage, R. Ross, W. Fichter, and A. Schleicher, "Closed-loop specifications for spacecraft control under micropropulsion constraints," *Journal of Guidance, Control, and Dynamics*, vol. 35, no. 5, pp. 1676–1681, 2012.